Check for updates

Fluorogenic platinum(IV) complexes as potential predictors for the design of hypoxia-activated platinum(IV) prodrugs†

Jevon W. Marsh,‡[a] Lina Hacker, ID ‡[b] Shitong Huang,[a] Marie H. C. Boulet,[a] Jhanelle R. G. White,[c] Louise A. W. Martin,[b] Megan A. Yeomans,[a] Hai-Hao Han, ID [d] Ismael Diez-Perez, ID [c] Rebecca A. Musgrave, ID [c] Ester M. Hammond ID *[b] and Adam C. Sedgwick ID *[a,c]

Hypoxia (low-oxygen) is one of the most common characteristics of solid tumours. Exploiting tumour hypoxia to reductively activate Pt(IV) prodrugs has the potential to deliver toxic Pt(II) selectively and thus overcome the systemic toxicity issues of traditional Pt(II) therapies. However, our current understanding of the behaviour of Pt(IV) prodrugs in hypoxia is limited. Here, we evaluated and compared the aryl carbamate fluorogenic Pt(IV) complexes, **CisNap** and **CarboNap**, as well as the previously reported **OxaliNap**, as potential hypoxia-activated Pt(IV) (HAPt) prodrugs. Low intracellular oxygen concentrations (<0.1%) induced the greatest changes in the respective fluorescence emission channels. However, no correlation between reduction under hypoxic conditions and toxicity was observed, except in the case for **CarboNap**, which displayed significant hypoxia-dependent toxicity. Other aryl carbamate Pt(IV) derivatives (including non-fluorescent analogues) mirrored these observations, where carboplatin(IV) derivative **CarboPhen** displayed a hypoxia-selective cytotoxicity similar to that of **CarboNap**. These findings underscore the need to perform extensive structure activity relationship studies on the cytotoxicity of Pt(IV) complexes under normoxic and hypoxic conditions.

Introduction

The FDA-approved platinum(II)-based anticancer agents cisplatin, carboplatin, and oxaliplatin are among the most widely used chemotherapeutics in oncology. Subtle structural modifications between these anticancer agents have been shown to have a broad impact on the corresponding reactivity, pharmacokinetics, and toxicity profiles, which is reflected in their clinical usage.[1] Unfortunately, the lack of tumour selectivity and resultant dose-limiting toxicity remains a fundamental problem for all three FDA-approved Pt(II) agents.[2,3] Pt(IV) anticancer agents typically display reduced off-target toxicities and enhanced drug bioavailability, and have emerged as attractive

alternatives to their Pt(II) congeners.[4] To date, several promising Pt(IV) candidates have been reported, notably satraplatin,[4] which reached phase 3 clinical trials.[4,5] Pioneering work from the groups of Gibson and Lippard, and among many others, have devoted their research efforts to understanding and developing Pt(IV) anticancer agents.[6–10] It is currently understood that Pt(IV) anticancer agents are prodrugs, which undergo intracellular reduction to afford the cytotoxic Pt(II) species along with the simultaneous release of two axial ligands from the Pt centre.[10] However, the redox chemistry of Pt(IV) prodrugs in a cellular context remains poorly understood, as well as how it might correlate with both cytotoxicity and tolerability.[11,12] Attempts to increase this understanding have centred around the development of fluorescence-based probes that allow the reduction of Pt(IV) to Pt(II) to be visualised in solution and in cells.[13–23] In this context, we recently developed two fluorogenic oxaliplatin-based Pt(IV) complexes, **OxaliRes** and **OxaliNap** that allowed the hypoxia-mediated reduction of Pt(IV) to Pt(II) to be monitored *via* the release of resorufin (Res) and naphthalimide (Nap-NH$_2$) fluorescent reporters, respectively (Fig. S1†).[24]

Hypoxia (low-oxygen) is a common characteristic of solid tumours. Targeting this cancer specific trait with hypoxia-activated Pt(IV) (HAPt) species that can act as either sensors and/or

[a]Chemistry Research Laboratory, University of Oxford, Mansfield Road, OX1 3TA, UK. E-mail: adam.sedgwick@kcl.ac.uk
[b]Department of Oncology, University of Oxford, Old Road Campus Research Building, Oxford, OX3 7DQ, UK. E-mail: ester.hammond@oncology.ox.ac.uk
[c]Department of Chemistry, King's College London, 7 Trinity Street, London, SE1 1DB, UK
[d]Shandong Laboratory of Yantai Drug Discovery, Bohai Rim Advanced Research Institute for Drug Discovery, Yantai, Shandong 264117, P. R. China
†Electronic supplementary information (ESI) available. See DOI: https://doi.org/10.1039/d4dt02173h
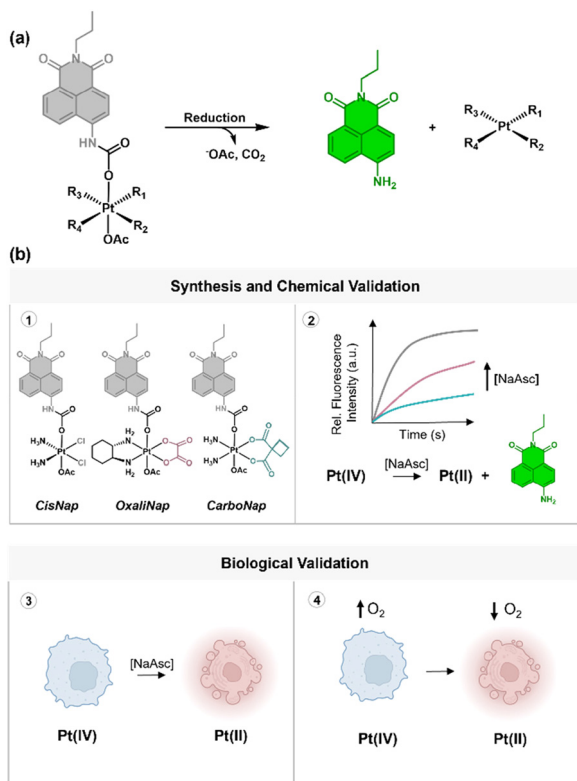‡These authors contributed equally to this work.

Fig. 1 (a) General schematic showing the reduction of a fluorogenic Pt (IV) complex to Pt(II) and release of the Nap-NH$_2$ (green) fluorophore; (b) the proposed stepwise workflow using fluorogenic Pt(IV) systems to aid the general development of a HAPt: (1) chemical synthesis; (2) chemical validation using NaAsc; (3) chemical reduction in cells using NaAsc; and (4) anaerobic reduction in cells using decreased oxygen concentrations.

prodrugs could afford cancer-selective agents that overcome the dose-limiting toxicity issues of Pt(II)-chemotherapy.[25–30] However, our current understanding of the design requirements for a HAPt is limited.[9,31–33] For these reasons, we have expanded our first generation fluorogenic Pt(IV) strategy based on oxaliplatin(II) to create Pt(IV) analogues of cisplatin(II) and carboplatin(II). To allow comparisons, we chose to incorporate a Nap-NH$_2$ fluorophore at the axial position to monitor the reduction of the Pt(IV) complexes *via* the release of the fluorophore (Fig. 1a). The resulting fluorescent HAPts investigated in this study (**OxaliNap**, **CisNap**, and **CarboNap**) are shown in Fig. 1b.

Results and discussion

CisNap and **CarboNap** were synthesised in a similar manner to our previously published protocol for **OxaliNap**.[24] The full synthetic procedures and characterisation of each compound can be found in the Scheme S1–S4†. First, we wanted to validate and compare the reduction profiles with the biological reductant sodium ascorbate (NaAsc) in PBS buffer solution (pH = 7.4). NaAsc is routinely used for determining the reduction profiles of Pt(IV) complexes *via* HPLC analysis.[34] Immediate

differences in the release of the Nap-NH$_2$ fluorophore were seen between **CisNap**, **OxaliNap**, and **CarboNap** using both UV-Vis and fluorescence spectroscopy. The incubation of each Pt(IV) complex with NaAsc (50 mM, 1 h) led to bathochromic shifts in the UV-vis absorbance (Fig. S2–S4†), where **CisNap** provided the greatest shift in absorption to 440 nm. **CarboNap** showed the least substantial changes and these shifts overlapped with the absorption spectrum of the free fluorophore Nap-NH$_2$ (λ_{max} = 440 nm, Fig. S5†). Despite clear literature precedent showing Nap-based systems as ratiometric fluorescent probes, no blue emission was observed for any Pt(IV) complex.[35,36] Clear differences in the emission profiles were observed in the absence and presence of NaAsc; minimal changes to the respective fluorescence emission intensities were seen in the absence of NaAsc over an 8 hour incubation period, a finding taken as evidence that all three complexes possessed good aqueous stability (Fig. S6–S14†).

The addition of NaAsc (0.25–16 mM) to **CisNap** (5 μM) led to a rapid (< 30 seconds) and dose-dependent increase in the fluorescence emission intensity at 545 nm (~50-fold change) – Fig. 2a and Fig. S15, S16.† In stark contrast, **CarboNap** and **OxaliNap** (5 μM) required longer incubation times (at least 1 h)
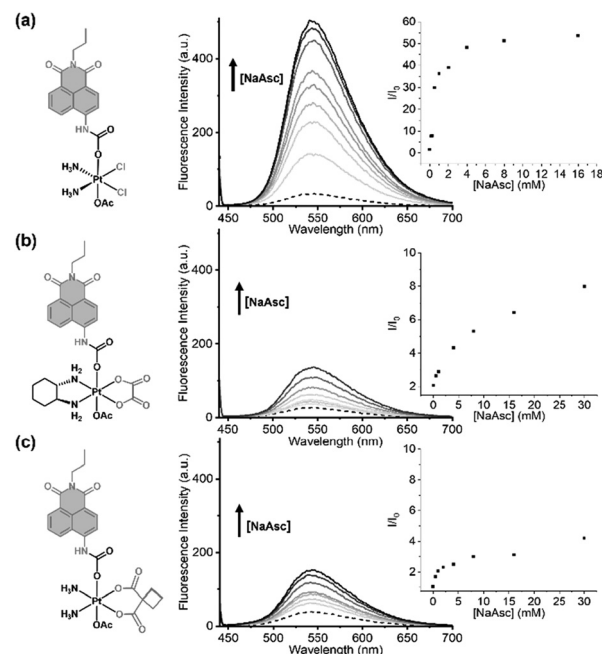

Fig. 2 (a) Chemical structure and fluorescence spectra of **CisNap** (5 μM) incubated with increasing concentrations of NaAsc for 1 h. Inset: relative fluorescence changes (I/I_0) at 545 nm as a function of NaAsc concentration (0, 0.25, 1, 2, 4, 8, and 16 mM); (b) chemical structure and fluorescence spectra of **OxaliNap** (5 μM) incubated with increasing concentrations of NaAsc for 1 h. Inset: relative fluorescence changes (I/I_0) at 545 nm as a function of NaAsc concentration (0, 0.5, 1, 2, 4, 8, 16, and 30 mM); (c) chemical structure and fluorescence spectra of **CarboNap** (5 μM) incubated with increasing concentrations of NaAsc for 1 h. Inset: relative fluorescence changes (I/I_0) at 545 nm as a function of NaAsc concentration (0, 0.5, 1, 2, 4, 8, 16, and 30 mM). All measurements were performed in PBS solution (pH = 7.4) with λ_{ex} = 430 nm. Slit widths: ex = 10 nm, em = 3.5 nm.

and greater NaAsc concentrations to achieve notable changes in fluorescence emission intensity (Fig. S17 and S18†). As seen in Fig. 2b and c, dose-dependent increases (0–30 mM) in the fluorescence emission intensities were observed with **OxaliNap** displaying a greater sensitivity to NaAsc-mediated reduction as compared to **CarboNap** (~8-fold change *vs.* 4-fold change, respectively). HPLC analyses confirmed the increase in fluorescence intensity expected upon the release of Nap-NH$_2$, thus providing indirect evidence for the reduction of the Pt(IV) center to Pt(II). Near-complete reduction of **CisNap** was seen *via* HPLC analysis after 2 hours incubation. **CarboNap** reduction monitored by HPLC proved slow when compared to **CisNap** and **OxaliNap** (Fig. S19–S21†). These observed trends in solution reduction rates correlated with the reduction potentials (cathodic peaks): **CarboNap** > **OxaliNap** > **CisNap** (−0.32/−0.17/−0.10 V *vs.* Ag/AgCl, respectively; see Fig. S22†), where **CarboNap**, with the most negative reduction potential, was hardest to reduce.

Before evaluating the intracellular reduction of these fluorogenic Pt(IV) systems, a selectivity assay was carried out with the aim of identifying any other potential reductants. Similar to other previously reported cisplatin(IV)-based systems,[37] other reductants such as glutathione (GSH) induced changes in the emission intensity for **CisNap**. However, **CarboNap** displayed a selective NaAsc-mediated fluorescence response similar to **OxaliNap**[24] (Fig. S23 and 24†). Minimal changes to the emission spectra of **CarboNap** and **OxaliNap** were seen when incubated with GSH concentrations ranging from 0–8 mM (Fig. S25 and S26†). NaAsc appears as the only effective reducing agent for **CarboNap** and **OxaliNap**. In light of these findings, we then compared the behaviour of each fluorogenic system in cancer cells.

A549 cells (lung adenocarcinoma ATCC) were chosen in this study as the model cell line due to the routine use of cisplatin and carboplatin in lung cancer treatment.[38,39] We wanted to confirm first that we could visualise changes in the fluorescence emission of each fluorogenic complex in cells using NaAsc. As expected, flow cytometry quantified the NaAsc-mediated increases in fluorescence emission (0.5 to 4 mM, 4 h incubation), thus confirming our ability to monitor Pt(IV) reduction in cancer cells (Fig. S27†). Next, we exposed A549 cells to the respective fluorogenic complexes, **CisNap**, **OxaliNap** and **CarboNap**, and incubated at different oxygen (O$_2$) concentrations, 21%, 2% and <0.1% O$_2$ for 16 hours before examining the relative fluorescence by microscopy (Fig. 3a). This oxygen-dependent study is crucial for understanding the hypoxia-selective activation of Pt(IV) prodrugs, as although 21% O$_2$ is universally referred to as "normoxic", oxygen concentrations in normal tissues average around ~6% O$_2$, and most tumour tissue oxygen levels are between 2–0% O$_2$.[40] In this oxygen dependent study, the greatest increases in fluorescence emission intensity were seen at low oxygen concentrations (2% and <0.1%) (Fig. 3a). Notably, a fluorescent signal at 21% O$_2$ was observed for **CisNap**. We attribute this latter observation to the high GSH concentrations reported to be found in cancer cells.[41] In comparison, minimal changes in
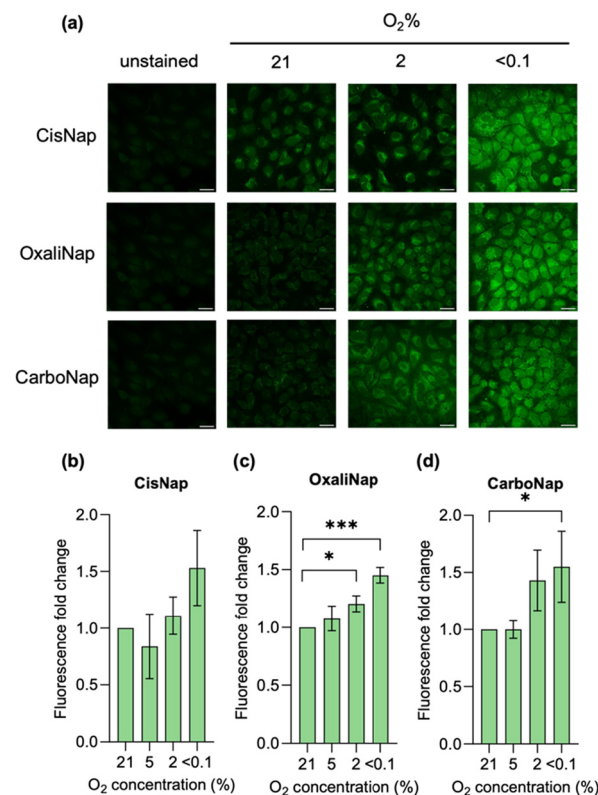

Fig. 3 (a) Representative fluorescence images of A549 cells treated with **CisNap**, **OxaliNap**, or **CarboNap** (10 μM) for 16 hours in the oxygen conditions indicated. Scale bar represents 12 μM. (b–d) Flow cytometry of A549 cells treated with 10 μM (b), **CisNap** (c) **OxaliNap** or (d) **CarboNap** for 16 hours in the oxygen conditions indicated. Fluorescence fold change of the geometric mean intensity is displayed. Error bars represent SD. Significance compared to normoxic control. *p < 0.05, and ***p < 0.001. n = 3.

fluorescence emission intensity were observed for **OxaliNap** and **CarboNap** at 21% O$_2$. Flow cytometry was subsequently used to quantify the changes in the fluorescence emission seen in cells following treatment with **CisNap**, **OxaliNap** and **CarboNap**. **OxaliNap** showed a significant increase in the fluorescence at 2% and <0.1% O$_2$ relative to those treated with **CarboNap** at <0.1% O$_2$ (Fig. 3b–d). Considered in concert, these data lead us to suggest that hypoxia results in reduction of the aryl carbamate fluorogenic Pt(IV) complexes and that this release mechanism should be operable in biological milieus.

Next, we sought to correlate the observed fluorescence responses (indicative of Pt(IV) reduction to Pt(II) complexes) with the cytotoxicity of **CisNap**, **OxaliNap**, and **CarboNap**. Nap-NH$_2$, the constituent fluorophore, was previously shown to be non-toxic.[24] Appreciating this, A549 cells were treated with **CisNap**, **OxaliNap** and **CarboNap** under normoxic conditions (21% O$_2$) and hypoxic conditions (<0.1% O$_2$, 16 hours) (Fig. 4). Cell survival was determined *via* a clonogenic assay. With the data in Fig. 3 providing support for the proposed hypoxia-mediated reduction of Pt(IV) to Pt(II), we anticipated that toxicity would only be observable at low oxygen concentrations.
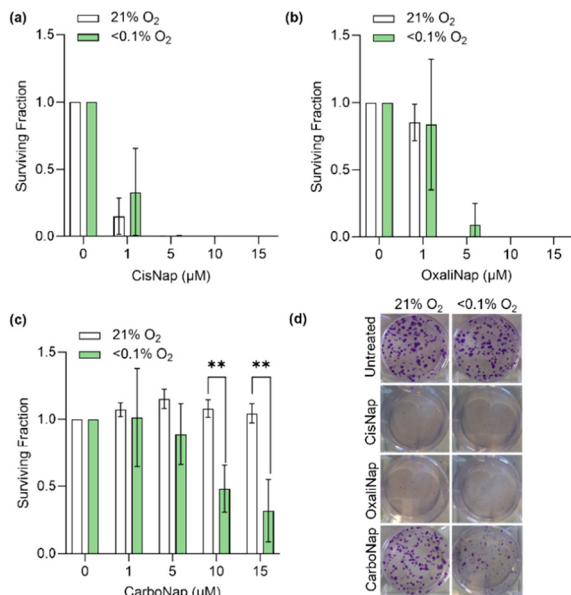
Fig. 4 A549 cells treated with the indicated concentrations of **CisNap**, **OxaliNap**, and **CarboNap** and exposed to <0.1% O$_2$ for 16 h. Cell survival was measured *via* clonogenic assay. Cell viability results for **CisNap** (a), **OxaliNap** (b), and **CarboNap** (c), are shown. (d) representative images from the colony survival assay are shown after treatment with 10 μM of each compound. Error bars represent SD **p < 0.01. n = 3.

Fig. 5 A549 cells treated with the indicated concentrations of carbo-platin(II), **CisPhen**, **OxaliPhen**, **CarboPhen** or **CarboBisOAc** and exposed to <0.1% O$_2$ for 16 h. Cell survival was measured *via* clonogenic assay. Cell viability results and chemical structures for (a) carboplatin, (b) **CisPhen** (c) **OxaliPhen**, and (d) **CarboPhen**. (e) Chemical structure of **CarboRes**. (f) Cell viability results and chemical structure for **CarboBisOAc**. Error bars represent SD **p < 0.01 n = 3.

However, both **CisNap** and **OxaliNap** (5 μM) led to loss of viability in normoxic and hypoxic environments, leading to the conclusion that the Pt(IV) complexes themselves are toxic at the indicated concentrations and exposure times. As noted in previous reports,[42] the rate of NaAsc- and, in this case, hypoxia-mediated reduction of the Pt(IV) complex does not correlate to the cytotoxicity. In contrast, **CarboNap** displayed excellent hypoxia-dependent cytotoxicity, highlighting its potential as a HAPt prodrug (Fig. 4c) and lead us to suggest that the release of carboplatin(II) is crucial for therapeutic efficacy. These findings emphasise the need to perform structure–activity relationship studies on Pt(IV) complexes under both normoxic and hypoxic conditions.

The hypoxia selectivity difference seen for **CarboNap** relative to the other two probes (**CisNap** and **OxaliNap**) is supported by the finding that carboplatin(II) also displays significant cytotoxicity towards A549 cells in both hypoxic and normoxic environments (Fig. 5a). We next investigated if the data obtained for each fluorogenic system extended to the non-fluorescent aryl carbamate Pt(IV) complexes. The aryl carbamate Pt(IV) complexes, **CisPhen**, **OxaliPhen**, and **CarboPhen** were synthesised following a literature reported protocol (Fig. 5).[34] HPLC analysis with and without the addition of NaAsc showed similar trends to the analogous fluorogenic systems where, responsiveness decreased: **CisPhen** > **OxaliPhen** > **CarboPhen** (Fig. S28–S31†). As seen in Fig. 5b and c, both **CisPhen** and **OxaliPhen** displayed toxicity in both normoxic and hypoxic conditions; again, this is consistent with these two species not needing to undergo hypoxia-mediated reduction to produce a
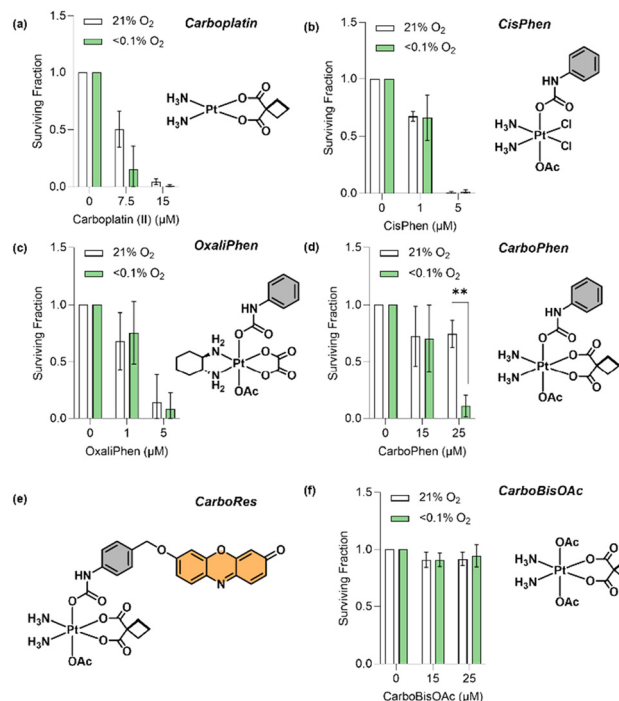
cytotoxic response. **CarboPhen** displayed a similar hypoxia-dependent toxicity to **CarboNap**. However, greater concentrations (>25 μM) of **CarboPhen** were required to induce hypoxia-dependent toxicity in A549 cells. Cyclic voltammetry experiments revealed that a subtle modification of the aryl carbamate functionality led to a significant difference in the reduction potential of **CarboPhen** (cathodic peak at −0.63 V *vs.* Ag/AgCl, Fig. S32†) and **CarboNap** (cathodic peak at −0.32 V *vs.* Ag/AgCl, Fig. S22†). In considering aryl carbamate-based carboplatin(IV) complexes as potential HAPt prodrugs, the self-immolative[15,43] strategy embodied in **CarboRes** (Fig. 5e) displayed a similar hypoxia-dependent toxicity (Fig. S33†); in contrast, the bis-acetate functionalised **CarboBisOAc** (Fig. 5f) was non-toxic in both normoxic and hypoxic conditions along with displaying a more negative reduction potential (cathodic peak at −0.77 V *vs.* Ag/AgCl, Fig. S34†) than **CarboPhen** and **CarboNap**. Building on these findings, preliminary density functional theory (DFT) calculations (see ESI – section 6†) on Pt(IV) complexes **CarboBisOAc**, **CarboPhen** and **CarboNap** (which differ only by the identity of one axial ligand) revealed an excellent linear correlation (R^2 > 0.98) between the observed reduction potential (cathodic peak) and the calculated energy of the lowest occupied molecular orbital (LUMO) (Fig. S62†).[44] Use of this correlation may permit the facile prediction of reduction potentials to help guide the future development of HAPt prodrugs.

Conclusions

To conclude, we have developed and utilised fluorogenic Pt(IV) complexes to identify and understand how hypoxia-mediated reduction of Pt(IV) to Pt(II) correlates to the corresponding toxicity profiles. As shown in the above data, hypoxia-mediated reduction and toxicity do not correlate for these oxaliplatin(IV) and cisplatin(IV) systems. The findings reported here lead us to suggest that the aryl carbamate carboplatin(IV) scaffold holds promise for the future development of HAPts. However, they also highlight the need to carry out cytotoxicity tests of Pt(IV) complexes under both normoxic and hypoxic conditions.

Data availability

The data supporting this article have been included as part of the ESI.†

Conflicts of interest

There are no conflicts to declare.

Acknowledgements

References

1 C. Zhang, C. Xu, X. Gao and Q. Yao, *Theranostics*, 2022, **12**, 2115–2132.

2 R. Oun, Y. E. Moussa and N. J. Wheate, *Dalton Trans.*, 2018, **47**, 6645–6653.

3 S. Dasari and P. B. Tchounwou, *Eur. J. Pharmacol.*, 2014, **740**, 364–378.

4 N. J. Wheate, S. Walker, G. E. Craig and R. Oun, *Dalton Trans.*, 2010, **39**, 8113–8127.

5 G. Thiabaud, G. He, S. Sen, K. A. Shelton, W. B. Baze, L. Segura, J. Alaniz, R. Munoz Macias, G. Lyness, A. B. Watts, H. M. Kim, H. Lee, M. Y. Cho, K. S. Hong, R. Finch, Z. H. Siddik, J. F. Arambula and J. L. Sessler, *Proc. Natl. Acad. Sci. U. S. A.*, 2020, **117**, 7021–7029.

6 T. Babu, A. Sarkar, S. Karmakar, C. Schmidt and D. Gibson, *Inorg. Chem.*, 2020, **59**, 5182–5193.

7 D. Gibson, *J. Inorg. Biochem.*, 2021, **217**, 111353.

8 D. Gibson, *Dalton Trans.*, 2016, **45**, 12983–12991.

9 N. Graf and S. J. Lippard, *Adv. Drug Delivery Rev.*, 2012, **64**, 993–1004.

10 T. C. Johnstone, K. Suntharalingam and S. J. Lippard, *Chem. Rev.*, 2016, **116**, 3436–3486.

11 G. Liu, Y. Zhang, H. Yao, Z. Deng, S. Chen, Y. Wang, W. Peng, G. Sun, M.-K. Tse, X. Chen, J. Yue, Y.-K. Peng, L. Wang and G. Zhu, *Sci. Adv.*, 2023, **9**, DOI: **10.1126/sciadv. adg5964**.

12 H. Yao, S. Chen, Z. Deng, M.-K. Tse, Y. Matsuda and G. Zhu, *Inorg. Chem.*, 2020, **59**, 11823–11833.

13 F.-K. Tang, J. Zhu, F. K.-W. Kong, M. Ng, Q. Bian, V. W.-W. Yam, A. K.-W. Tse, Y.-C. Tse and K. C.-F. Leung, *Chem. Commun.*, 2020, **56**, 2695–2698.

14 H. Yao and G. Zhu, *Dalton Trans.*, 2022, **51**, 5394–5398.

15 V. E. Y. Lee, Z. C. Lim, S. L. Chew and W. H. Ang, *Inorg. Chem.*, 2021, **60**, 1823–1831.

16 D. Montagner, S. Q. Yap, W. H. Ang, D. Montagner, S. Q. Yap and W. H. Ang, *Angew. Chem., Int. Ed.*, 2013, **52**, 11785–11789.

17 E. J. New, R. Duan, J. Z. Zhang and T. W. Hambley, *Dalton Trans.*, 2009, 3092–3101, DOI: **10.1039/B821603G**.

18 J. X. Ong, C. S. Q. Lim, H. V. Le and W. H. Ang, *Angew. Chem., Int. Ed.*, 2019, **58**, 164–167.

19 S. Chen, Q. Zhou, K.-Y. Ng, Z. Xu, W. Xu and G. Zhu, *Inorg. Chem. Front.*, 2024, **11**, 3085–3118.

20 L. Mitchell, C. Shen, H. C. Timmins, S. B. Park and E. J. New, *ACS Sens.*, 2021, **6**, 1261–1269.

21 S. Huang, J. W. Marsh, J. R. G. White, T. Q. Ha, S. A. Twigger, I. Diez-Perez and A. C. Sedgwick, *New J. Chem.*, 2024, **48**, 7548–7551.

22 J. J. Wilson and S. J. Lippard, *Inorg. Chim. Acta*, 2012, **389**, 77–84.

23 Y. Song, K. Suntharalingam, J. S. Yeung, M. Royzen and S. J. Lippard, *Bioconjugate Chem.*, 2013, **24**, 1733–1740.

24 M. H. C. Boulet, H. R. Bolland, E. M. Hammond and A. C. Sedgwick, *J. Am. Chem. Soc.*, 2023, **145**, 12998–13002.

25 Z. Chen, F. Han, Y. Du, H. Shi and W. Zhou, *Signal Transduction Targeted Ther.*, 2023, **8**, 70, DOI: **10.1038/ s41392-023-01332-8**.

26 E. M. Hammond, M. C. Asselin, D. Forster, J. P. O'Connor, J. M. Senra and K. J. Williams, *Clin. Oncol.*, 2014, **26**, 277–288.

27 A. L. Harris, *Nat. Rev. Cancer*, 2002, **2**, 38–47.

28 F. W. Hunter, B. G. Wouters and W. R. Wilson, *Br. J. Cancer*, 2016, **114**, 1071–1077.

29 Y. Li, L. Zhao and X. F. Li, *Front. Oncol.*, 2021, **11**, 700407.

30 A. Sharma, J. F. Arambula, S. Koo, R. Kumar, H. Singh, J. L. Sessler and J. S. Kim, *Chem. Soc. Rev.*, 2019, **48**, 771–813.

31 Q. Cao, D. J. Zhou, Z. Y. Pan, G. G. Yang, H. Zhang, L. N. Ji and Z. W. Mao, *Angew. Chem., Int. Ed.*, 2020, **59**, 18556–18562.

32 M. Maji, I. Bhattacharya, S. Acharya, M. P. Chakraborty, A. Gupta and A. Mukherjee, *Inorg. Chem.*, 2021, **60**, 4342–4346.

33 E. Schreiber-Brynzak, V. Pichler, P. Heffeter, B. Hanson, S. Theiner, I. Lichtscheidl-Schultz, C. Kornauth, L. Bamonti, V. Dhery, D. Groza, D. Berry, W. Berger, M. Galanski, M. A. Jakupec and B. K. Keppler, *Metallomics*, 2016, **8**, 422–433.

34 S. Chen, H. Yao, Q. Zhou, M. K. Tse, Y. F. Gunawan and G. Zhu, *Inorg. Chem.*, 2020, **59**, 11676–11687.

35 C. Wynne and R. B. P. Elmes, *Front. Chem.*, 2024, **12**, DOI: **10.3389/fchem.2024.1418378.**

36 M. H. Lee, J. Y. Kim, J. H. Han, S. Bhuniya, J. L. Sessler, C. Kang and J. S. Kim, *J. Am. Chem. Soc.*, 2012, **134**, 12668–12674.

37 C. J. Adams and T. J. Meade, *Chem. Sci.*, 2020, **11**, 2524–2530.

38 G. Y. Ho, N. Woodward and J. I. G. Coward, *Crit. Rev. Oncol. Hematol.*, 2016, **102**, 37–46.

39 J. Lokich and N. Anderson, *Ann. Oncol.*, 1998, **9**, 13–21.

40 S. R. McKeown, *Br. J. Radiol.*, 2014, **87**, 20130676.

41 L. Kennedy, J. K. Sandhu, M. E. Harper and M. Cuperlovic-Culf, *Biomolecules*, 2020, **10**, DOI: **10.3390/biom10101429**.

42 S. Choi, C. Filotto, M. Bisanzo, S. Delaney, D. Lagasee, J. L. Whitworth, A. Jusko, C. Li, N. A. Wood, J. Willingham, A. Schwenker and K. Spaulding, *Inorg. Chem.*, 1998, **37**, 2500–2504.

43 A. G. Gavriel, M. R. Sambrook, A. T. Russell and W. Hayes, *Polym. Chem.*, 2022, **13**, 3188–3269.

44 J. J. Wilson and S. J. Lippard, *Inorg. Chem.*, 2011, **50**, 3103–3115.